Eur. Phys. J. D **24**, 157–160 (2003)
DOI: 10.1140/epjd/e2003-00120-y

THE EUROPEAN PHYSICAL JOURNAL D

Dynamics of free and embedded lead clusters in intense laser fields

T. Döppner, S. Teuber, Th. Diederich, Th. Fennel, P. Radcliffe, J. Tiggesbäumker[a], and K.H. Meiwes–Broer

Fachbereich Physik, Universität Rostock, 18051 Rostock, Germany

Received 10 September 2002
Published online 3 July 2003 –

Abstract. Lead clusters are exposed to strong femtosecond light pulses. The dependence of the recoil energy on the charge state of the atomic ion is now investigated using a new detection setup, *i.e.*, a Thomson analyser. First results show that in contrast to laser–induced overdense plasmas at surfaces the recoil energy distribution appears much narrower. Comparing free lead clusters with lead clusters embedded in large helium droplets, the charging dynamics show distinct differences on the femtosecond time scale. In the embedded case the maximum ionization enhancement is reached earlier.

PACS. 36.40.Gk Plasma and collective effects in clusters – 52.50.Jm Plasma production and heating by laser beams (laser-foil, laser-cluster, etc.) – 67.40.Yv Impurities and other defects

1 Introduction

When short, intense laser pulses are focused onto nanometer–sized objects, the interaction is far from equilibrium and highly non–linear effects govern the dynamics. In the region above 10^{13} W/cm^2 the laser field is strong enough to lower the ionization barrier and the charging of atoms is possible. A good estimate for the threshold laser intensity I_{th} required to charge an atom is given by the barrier suppression model. For singly charged Pb atoms ($I_P = 7.4$ eV) the model gives a value of $I_{th} = 1.2 \times 10^{13}$ W/cm^2. This threshold intensity increases dramatically if one wants to remove one electron per atom in a cluster with N atoms. In this case I_{th} can be estimated using the conducting sphere model to be

$$I_{th}[\mathrm{W/cm^2}] = \frac{4 \times 10^9}{Z^2} \left(WF + \frac{e^2}{4\pi\epsilon_o r_s} \frac{Z - 1/2}{N^{1/3}} \right) \quad (1)$$

where Z is the final charge state, WF the work function of the material and r_s its Wigner-Seitz radius. For comparison with the free singly charged lead ion a Pb_{50} cluster is considered to be charged to $Z = 50$. In this case, equation (1) gives a threshold intensity of $I_{th} = 1.2 \times 10^{15}$ W/cm^2. This is substantially higher than the value for an isolated atom, since the laser field also has to deliver the coulomb energy of the charged system. However, the observed ionic charge states after interaction with intense laser pulses are higher in the case of nanoparticles and clusters than for atoms, see, *e.g.*, reference [1]. This strong light-matter interaction is attributed to collective electron excitations, especially the plasmon resonance of the metal cluster [2].

So far most experiments have focused on large rare gas nanoparticles [3] which are relatively easy to produce as intense beams. Highly charged ions, energetic electrons and X–rays emitted from these particles have been observed, and it was shown that the cluster beam absorbs nearly 100% of the incident light. Whereas in rare gas clusters a nanoplasma must first be created which needs a laser field of at least 10^{13} W/cm^2, in small metal systems plasmons can be excited even with nanosecond light pulses [4]. It has been shown that this circumstance can be used to generate highly charged ions from platinum [1] and lead clusters [5,6]. Intense laser light interacting with clusters and nanoparticles might also be of technological relevance in order to construct a debris–free plasma light source in the deep VUV [7].

Since the excitations are in the strong non–linear regime calculations become extremely complex when trying to describe the laser-matter interaction correctly. There is a continuing debate as to whether or not the expansion of the ionized cluster system is governed by pure Coulomb forces or by the nanoplasma temperature (hydrodynamic expansion) [3]. It was calculated that the maximum ionic recoil energy should show a distinct signature since Coulomb interaction would give the well-known quadratic dependence on the charge state, whereas in the hydrodynamic case a linear dependence is expected [8]. In order to investigate this fundamental question we have built an experimental setup for simultaneously measuring ion charge state and energy. It turns out that the energy distribution of the ions as a function of the charge state

[a] e-mail: tiggesbaeumker@physik.uni-rostock.de

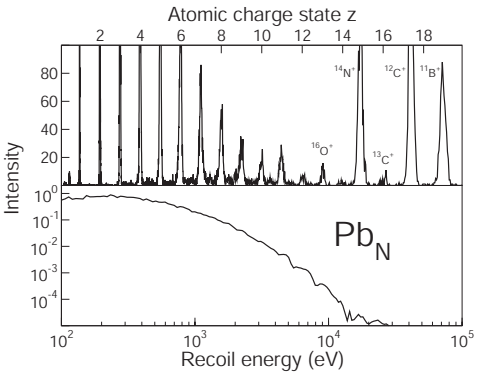

Fig. 1. Charge distribution as obtained in the mass spectrometer (top) and recoil energy spectrum (bottom) of the ionic fragments of small lead clusters exposed to intense laser light pulses with a width of 600 fs @ 800 nm, and 1.3×10^{15} W/cm^2.

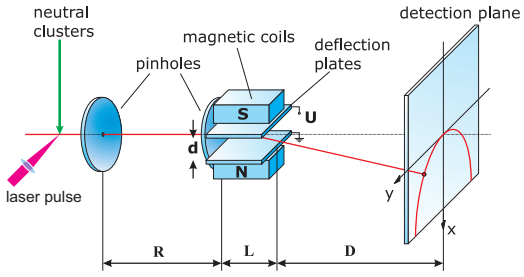

Fig. 2. Operation principle of the Thomson analyzer. A multi channel plate (MCP) detector with an imaging system serves to record the ions. With this setup the ion energies and charge states are simultaneously analyzed.

is rather narrow and that the maximum recoil energy depends almost linearly on the charge state.

In a second study we focus on the question whether the absorption mechanism changes when the clusters are embedded in helium droplets. In particular the charging dynamics has been investigated on a femtosecond time scale with the pump–probe technique, which will be compared for both the embedded and the free clusters.

2 Free lead clusters

From former experiments we know that the interaction of free Pb_N with an intense femtosecond laser field leads to the emission of highly charged atomic ions with high recoil energies [1,9]. As an example Figure 1 shows a typical mass and recoil energy spectrum for a laser intensity of 1.3×10^{15} W/cm^2 @ 800 nm and 600 fs pulse length. At these specific laser conditions the maximum kinetic energy ranges up to about 10 keV and the maximum charge state reaches $Z_{max} = 14$. Both values can be maximized by varying the pulse width whilst keeping everything else constant. In particular for lead, the highest observed recoil energy (180 keV [9]) is obtained with the shortest pulse (140 fs), whereas the maximum charge state ($Z_{max} = 28$ [5]) is recorded when the compressor in the amplifier is detuned to a pulse width of about 1 ps.

Calculating the recoil energy spectra within a molecular dynamics simulation reveals that the kinetic energy of the ions is extremely sensitive to the ion–ion distances [9]. As expected, a maximum in the potential energy is achieved when the ions are as close as possible, *i.e.* when they still have the density of the neutral cluster. Thus, in order to maximize the recoil energy, ionization has to occur before the ion dynamics sets in, *i.e.* within the first 100 fs.

Next, we will discuss that the charge build–up in the cluster strongly depends on the ion and electron kinetics, since the most prominent absorption in metals proceeds *via* the plasmon resonance. Generally this is located in the UV region and thus far away from the photon energy (1.54 eV) of the driving laser field. During the leading edge of the laser pulse the Coulomb explosion of the cluster is initiated by optical field ionization. Due to the following expansion the charge density and hence the energy of the collective resonance will decrease. After about half a picosecond plasmon and photon energies come into resonance and thus strong ionization *via* multi–plasmon absorption can occur [1,5].

Thomson spectroscopy

In order to measure simultaneously the energy and the charge of the ions expelled from an exploding cluster we have built a spectrometer based on the method first used by Thomson [10]. The general working principle of the Thomson analyzer is illustrated in Figure 2. It consists of parallel electric and magnetic fields, followed by a field free drift zone in connection with a position sensitive detector. Detailed information of our setup will be given in a forthcoming contribution. Assuming homogeneous E and B fields and small deflection angles, the coordinates (x, y), where ions with a given charge to mass ratio Z/m and a velocity v_o hit the detector, are given by $x = \alpha_E ZeE/(mv_o^2)$ and $y = \alpha_B ZeB/(mv_o)$ where $\alpha_E = \alpha_B = L(D + L/2)$ are constants which depend on the geometry. Ions with a given mass to charge ratio trace a parabola on the detection screen $x = (\alpha_E E/\alpha_B^2 eB^2)(m/z)y^2$. The origin is defined by the projection of the interaction area through two pinholes onto the screen.

In Figure 3 a resulting recoil energy spectrum is shown for Pb^{Z+}. These ions emerge from exploding lead clusters which are irradiated by 800 fs laser pulses having a focal intensity of 1.8×10^{15} W/cm^2 at 800 nm. To obtain such a spectrum the CCD signal has to be transformed into energy and charge space. Due to the restricted resolution of the analyzer it is not possible yet to fully resolve single ionic charge states and thus the ion intensity curve is smeared out. As shown in Figure 3 most ions have a charge state between $Z = 2$ and $Z = 10$ with kinetic energies in the range of $E = 0.5$–4 keV.

To get more detailed information, the energy distribution for each charge state is extracted. A closer look at the

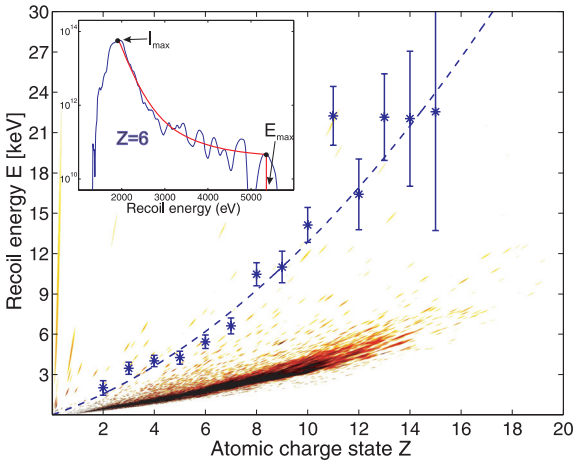

Fig. 3. Intensity plot of the ion recoil energy distribution *versus* charge state after transformation from a raw Thomson spectrum. Most of the intensity is concentrated in the shaded contours. A detailed analysis (see the energy distribution in the inset) of the high energy tails yields the maximum energies E_{max} as indicated by the asterisks.

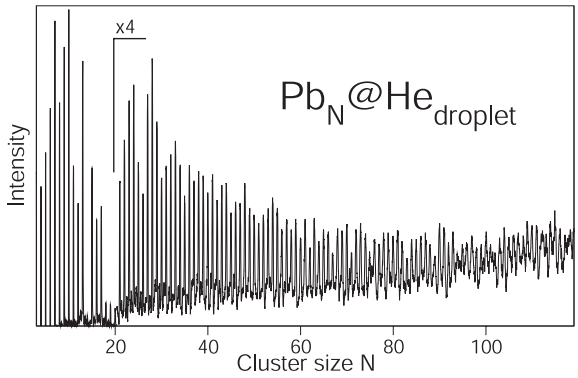

Fig. 4. Abundance spectrum of Pb clusters produced in a pick up process of Pb atoms by large He-droplets and ionized by 4.66 eV laser light.

individual recoil spectra reveals that they are far from being symmetric. Indeed, high energy tails, with low intensities, range up to values which are depicted by the asterisks. These were chosen to have a thousandth of the maximum intensity I_{max} (see inset of Fig. 3). A parabola is fitted to the maximum energy values E_{max} which are weighted by I_{max}. Clearly, the fit curve shows quadratic contributions. Following earlier discussions [6] a linear E_{max}/Z dependence should point to a hydrodynamic expansion, whereas a Coulomb explosion should lead to $E_{max} \propto Z^2$.

However, a systematic analysis shows, that the situation might not be that simple. If the expansion is governed exclusively by Coulomb forces then the maximum recoil energies would have a quadratic dependence on the charge state, $E_{max} \propto Z^2/R$, where R is the cluster radius. If the ionization does not occur instantaneously the actual radius might become important. This question motivated molecular dynamics simulations which takes the experimental measured charging dynamics into account. Based only on a Coulomb–like expansion these calculations can indeed qualitatively reproduce the results shown in Figure 3. Hence a linear dependence between maximum recoil energy and charge state does not necessarily mean that the expansion is governed by hydrodynamic forces. This is in partial disagreement to the conclusion of Schmidt *et al.* [6].

3 Metal clusters embedded in helium droplets

So far free clusters have been subject of the investigation. A surrounding medium, however, might influence the expansion dynamics. In order to perform these kind of studies metal clusters are embedded into superfluid helium droplets. Such systems are produced with a setup as described in reference [11]. In brief: helium droplets with a mean diameter of about 600 Å are formed in a supersonic expansion of cold helium gas (8 K) through a tiny nozzle. When the droplets traverse an oven filled with lead, they pick up atoms, which may coagulate to form clusters inside the droplets. To give an impression of the size range produced with this experimental setup, Figure 4 shows a mass spectrum of Pb_N upon ionization with nanosecond laser pulses of 266 nm. Bare lead clusters are found with up to 120 atoms. In the small size range the distribution has a distinct structure with a pronounced maximum at Pb_{13} and a nearly missing Pb_{14}. For larger clusters a smoother size distribution is recorded.

For the intense laser field experiments the setup is similar as for the free clusters, *i.e.* intensities of up to 2×10^{16} W/cm^2 @ 800 nm can be applied. In a first set of measurements the pulse width was varied from 120 fs to 8 ps while keeping the energy per pulse constant. Similar to free metal clusters the maximum charge state is enhanced for longer pulse widths. However, with embedded Pb_N the highest charge state emerges at a pulse width of 400 fs. This is considerably shorter compared to the free cluster case, where the maximum enhancement occurs around 1 ps [5]. The maximum charge state for Pb_N in the droplets is with $Z = 12$ clearly lower than the value found for free clusters ($Z = 28$ [5], $Z = 26$ [6]). At present we explain this difference by electron transfer from neutral or singly ionized helium atoms into free energy levels of the high Z lead ions.

To analyze the dynamics of the processes leading to ejection of highly charged ions and to compare the situation for free and embedded metal clusters, pump–probe experiments are performed. The optical delay is generated by a Mach–Zehnder interferometer, which typically delivers pulses of 2.5 mJ at a width of 100 fs @ 800 nm. By focussing the light with a 40 cm lens the clusters are exposed to intensities of up to 2.7×10^{15} W/cm^2. For each delay a time-of-flight mass spectrum is recorded, which is averaged typically over 2000 laser shots. Those channels of the TOF–spectrum which can be assigned to a certain charge state are integrated and plotted with respect to the optical delay. As an example Figure 5 shows the results of the Pb^{6+} intensities for free and embedded Pb clusters.

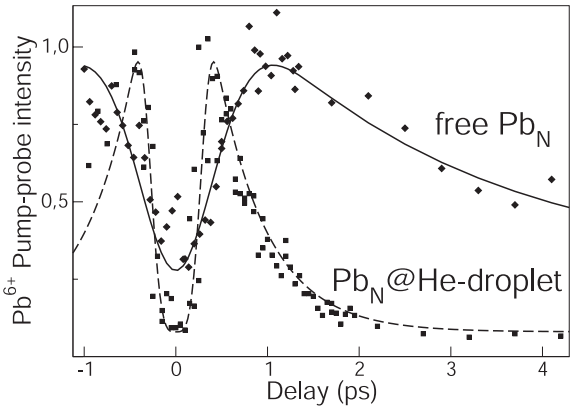

Fig. 5. Normalized pump–probe signal of Pb^{6+} from the Coulomb explosion of free (open symbols and the solid line) and embedded (bold symbols and the broken line) Pb clusters with respect to the optical delay. The curves are fits to serve as a guide to the eye.

Clearly, in both cases a zero or very short delay only yields a low count rate. The helium droplet signal rises significantly earlier. Thus the optimum condition for the charging enhancement is reached faster than for free clusters. The reasons for this behavior are still under discussion. In our opinion the charging enhancement is due to the occurrence of a resonance condition between the photon energy of the laser (1.54 eV) and the plasmon of the cluster, which shifts to lower values as the particle expands [1]. At first sight, within this picture of a multiplasmon excitation mechanism a contrary time dependency would be expected, since the expansion of the embedded Pb_N could be decelerated by the helium environment. This in turn would increase the time required to reach the state where the charge density matches the resonance condition.

On the other hand, the initial charging could be much more effective inside the droplet. Since simultaneous partial ionization of the surrounding helium is likely much more electrons perform a quiver motion in the laser field, leading to a higher electron–atom collision rate. This could cause a higher initial charging of the lead cluster and thus a faster expansion which indeed would lead to an earlier resonance between the photon and the plasmon energies.

Furthermore, it might be possible that the nature of the collective resonance is different in the droplet environment. It is well-known that the helium is repelled by electrons which results in the formation of bubbles with a diameter of 17 Å in its ground state. Leiderer *et al.* have even observed multi–electron bubbles which are stable due to the counterplay of the Coulomb–pressure of the escaping electrons and the surface tension of the helium environment [12]. However, the time scale for bubble formation, which was calculated by Rosenblit *et al.* to be 4 ps [13], is too long to explain the measured time dependency.

Nevertheless the helium environment might serve as a cage for slow electrons which thereby stay in the vicinity of the metal core. This would lead to an enhanced polarizability of the metal cluster which in turn causes a significant red–shift of the collective resonance. A related behavior is known from simple jellium cluster physics where the electron spill–out decreases the plasmon energy by about 10% in the case of sodium.

Similar results obtained for silver clusters embedded in helium droplets suggest that the observed behavior can be generalized to metal clusters. The results of these experiments along with molecular dynamics simulations will be presented in a forthcoming publication.

We would like to express our thanks and gratitude to the group of Professor Toennies, who designed and constructed the helium droplet machine. The authors acknowledge financial support from the Sonderforschungsbereich 198 and the Deutsche Forschungsgemeinschaft.

References

1. L. Köller, M. Schumacher, J. Köhn, S. Teuber, J. Tiggesbäumker, K.-H. Meiwes-Broer, Phys. Rev. Lett. **82**, 3783 (1999)
2. F. Calvayrac, P.-G. Reinhard, E. Suraud, C.A. Ullrich, Phys. Rep. **337**, 493 (2000)
3. E.M. Snyder, S.A. Buzza, A.W. Castleman Jr, Phys. Rev Lett. **77**, 3347 (1996); Y.L. Shao, T. Ditmire, J.W.G. Tisch, E. Springate, J.P. Marangos, M.H.R. Hutchinson, Phys. Rev. Lett. **77**, 3343 (1996); A. McPherson, B.D. Thompson, A.B. Borisov, K. Boyer, C.K. Rhodes, Nature **370**, 631 (1994); T. Ditmire, R.A. Smith, J.W.G. Tisch, M.H.R. Hutchinson, Phys. Rev. Lett. **78**, 3121 (1997)
4. J. Tiggesbäumker, L. Köller, K.-H. Meiwes-Broer, A. Liebsch, Phys. Rev. A **48**, R1749 (1993)
5. T. Döppner, S. Teuber, M. Schumacher, J. Tiggesbäumker, K.H. Meiwes-Broer, Appl. Phys. B **71**, 357 (2000)
6. M.A. Lebeault, J. Viallon, J. Chevaleyre, C. Ellert, D. Normand, M. Schmidt, O. Sublemontier, C. Guet, B. Huber, Eur. Phys. J. D **20**, 233 (2002)
7. E. Parra, I. Alexeev, J. Fan, K.Y. Kim, S.J. McNaught, H.M. Milchberg, Phys. Rev. E **62**, R5931 (2000)
8. S. Dobosz, M. Schmidt, M. Perdrix, P. Meynadier, O. Gobert, D. Normand, K. Ellert, T. Blenski, A.Ya Faenov, J. Exp. Theor. Phys. **88**, 1122 (1999)
9. S. Teuber, T. Döppner, T. Fennel, J. Tiggesbäumker, K.H. Meiwes-Broer, Eur. Phys. J. D **16**, 59 (2001)
10. J.J. Thomson, Phil. Mag., Series 6 **13**, 561 (1907)
11. A. Bartelt, J.D. Close, F. Federmann, N. Quaas, J.P. Toennies, Phys. Rev. Lett. **77**, 3525 (1996)
12. U. Albrecht, P. Leiderer, Europhys. Lett. **3**, 705 (1987)
13. M. Rosenblit, J. Jortner, Phys. Rev. Lett. **75**, 4079 (1995)